American Mineralogist, Volume 90, pages 1062–1071, 2005

X-ray Rietveld refinement and FTIR spectra of synthetic (Si,Ge)-richterites

KANA SENDA,[1] KIYOTAKA ISHIDA,[1,*] AND DAVID M. JENKINS[2]

[1]Department of Environmental Changes, Graduate School of Social and Cultural Studies, Kyushu University, 4-2-1 Ropponmatsu, Chuo-ku, Fukuoka 810-8560, Japan
[2]Department of Geological Sciences and Environmental Studies, Binghamton University, Binghamton, New York 13902-6000, U.S.A.

ABSTRACT

Richteritic amphiboles in which tetrahedral Si was substituted for Ge were synthesized using internally heated gas vessels at 795~905 °C and 720~756 MPa. There is complete solid-solution between ^{IV}Si and ^{IV}Ge richterite. The materials were characterized by scanning electron microscopy (SEM), high-resolution transmission electron microscopy (HRTEM), analytical transmission electron microscopy (AN-TEM), electron microprobe analysis (EMPA), X-ray diffraction (XRD) Rietveld structure refinement, and Fourier-transform infrared spectroscopy (FTIR). X-ray diffraction data for the richterites indicate that, with increasing Ge replacement for Si, all cell parameters (= *a*, *b*, *c*, and β) increase linearly and the rotation angle of the double chains increases. Refinement of the Ge and Si contents at the tetrahedral sites indicate that the Ge content at the T2 site is greater than at the T1 site for amphiboles of intermediate composition. Deuteration experiments were also made for the purpose of FTIR analysis. Infrared OH/OD-stretching bands attributed to the configurations (MgMgMg)-OH/OD-^{A}Na(K) and (MgMgMg)-OH/OD-^{A}□ (□ = vacancy) were observed. The frequency of the former bands decreases linearly with increasing Ge content, while the frequency and the intensity of the latter band decreases with increasing Ge content. Both sets of OH/OD-stretching bands show a continuous or one-mode change along the compositional join without any identifiable fine structure, indicating a lack of any short-range ordering within the tetrahedral double chain. The Si-O (at 1200~800 cm^{-1}) and Ge-O (at 950~700 cm^{-1}) stretching bands show similar continuous down-frequency shifts, and interactions of their modes are very small. The chain deformation bands of Si•Si-O, Si•Ge-O, and Ge•Ge-O are observed at 770~650, 660~590, and 590~510 cm^{-1}, respectively, with the frequency range of their absorption bands becoming narrower with increasing Ge content. A weak and broad OH librational band appears at 600 cm^{-1} in Si-richterite. With increasing Ge for Si substitution this band shifts upward in frequency, becoming centered at 650 cm^{-1} in Ge-richterite, which is the opposite behavior to the downward frequency shift of the OH/OD-stretching vibrations. The most notable aspect of this study is the continuous changes that are observed in the structure (cell dimensions, bond distances) and infrared spectra of richterite with replacement of Si by Ge. The only long-range ordering effect that was clearly observed was the preference of Ge over Si at the tetrahedral T2 site for intermediate compositions. Evidence for short-range ordering that can be observed in the OH-stretching region of the Ge-analogue of talc was not observed in Ge-richterite.

INTRODUCTION

Although many crystal-chemical studies have been made of synthetic richterites with various ionic substitutions (Charles 1975; Robert et al. 1989, 1993; Pawley et al. 1993; Della Ventura et al. 1993a, 1993b, 1996a, 1996b, 1997, 1999; Hawthorne et al. 1997; Melzer et al. 2000), studies of Ge replacing Si in amphiboles of richterite (or any) composition have not been previously reported. As silicon (atomic number = 14, ^{IV}Si = 0.26 Å; Shannon 1976) and germanium (atomic number = 32, ^{IV}Ge = 0.40 Å) have similar chemical characteristics but different physical properties, numerous germanates have been investigated as silicate analogues of mantle minerals for obtaining crystal-chemical and pressure-temperature (*P-T*) stability information. Large differences in the physical properties of Ge and Si are useful for obtaining crystal chemical information for synthetic amphiboles through the X-ray powder diffraction Rietveld method and by FTIR spectroscopy. The X-ray scattering power for Ge is 2.29 (= 32/14) times larger than Si and a large chemical shift is expected for infrared spectra arising from the mass effect (Ge is 2.58 times heavier than Si). Some assignments of the bands in the mid-infrared spectra of amphiboles were made by Lazarev (1972), Gillet et al. (1989), Ishida (1990), and Andrut et al. (2000); however, there are many features of these spectra still needing investigation.

We have performed hydrothermal syntheses of Ge-substituted Si-richterites for the purpose of determining (1) the effects that cation substitutions into the tetrahedral chain will have on the structure (cell dimensions and bond distances), (2) the presence of any long-range Si-Ge ordering at the tetrahedral sites (by XRD), (3) the presence of any short-range Si-Ge ordering (by FTIR), and (4) the effects of Ge substitution for Si on the lattice-vibration region of the FTIR spectra. In addition, deuteration experiments were performed to help identify any fine structure in the hydroxyl-stretching region (3800–3600/2800–2600 cm^{-1}) and to identify OH oscillations (librations) that occur in the lattice vibration range (1300–400 cm^{-1}) of the FTIR spectra.

* E-mail: kiyota@rc.kyushu-u.ac.jp

0003-004X/05/0007–1062$05.00/DOI: 10.2138/am.2005.1644

EXPERIMENTAL AND ANALYTICAL METHODS

Synthesis experiment

Experiments at 795~905 °C and 720~756 MPa were done in internally heated gas vessels at Binghamton University, using Ar as a pressure medium (Table 1). The samples were made from mixtures of reagent-grade oxides (MgO, Al_2O_3, SiO_2, GeO_2) and carbonates (Na_2CO_3, K_2CO_3, $CaCO_3$). The starting materials were mixed together and decarbonated by roasting for a few minutes at roughly 900 °C in air, and then sealed in 3.8 mm outer-diameter (OD) × 3.5 mm inner-diameter (ID) × 15 mm length Pt capsules with about 10 wt% distilled water.

Deuteration experiments were performed at about 600 °C, 200 MPa, and 1 day duration in cold-seal externally heated Tuttle-type vessels at Kyushu University. A double capsule method similar to that used by Jenkins (1989) was used to obtain a higher degree of deuteration: a welded inner Ag tube (3.0 mm OD × 2.7 mm ID × 25 mm length), which contained about 20 mg of synthetic amphibole and 20 mg 99.9% D_2O, was put into an outer Au tube (4.5 mm OD × 4.2 mm ID × 35~40 mm length) with 50 mg D_2O.

SEM, TEM, and AN-TEM analyses

Synthesized materials were examined using a scanning electron microscope (SEM), model JEOL JSM-5600 operated at Kyushu University, after the powdered specimens were coated with gold in an evaporative coater. High-resolution transmission-electron microscopy (HRTEM) analyses were done at the Research Laboratory for High Voltage Electron Microscopy, Kyushu University, with a JEOL JEM-4000EX microscope operated at 400 kV accelerating voltage and fitted with a top-entry goniometer. Samples were prepared by dispersing the crystal aggregates onto Cu grids coated with holey carbon support film. Selected-area electron-diffraction (SAED) patterns and high-resolution (HRTEM) images were obtained for about 20 crystals from each sample. Selected crystals were imaged with the electron beam perpendicular to the $\boldsymbol{b}^*$ axis allowing determination of the chain-multiplicity fault type and abundance. The compositions of the crystals were obtained by analytical TEM techniques (AN-TEM) using a JEOL JEM-2010HT equipped with an Oxford ISIS energy-dispersive spectroscopy (EDS) system at the Center for Instrumental Analysis at Nagasaki University. About 20 crystals from each sample were analyzed with 200 kV accelerating voltage and 100 s counting times. Electron microprobe analyses were obtained for the high-pressure series of samples at Binghamton University using a JEOL 8900 operated at 15 kV and 10 nA beam current using wavelength-dispersive spectroscopy (WDS) and the ZAF correction scheme. The standards for Na, K, Ca, Mg, Si, and Ge were albite, orthoclase, diopside, MgO, SiO_2, and GeO_2 glass, respectively.

X-ray Rietveld analysis

Powder diffraction data were collected with a Rigaku Rint-2100V diffractometer using curved-graphite monochromatized Cu$K\alpha$ X-rays and operating at 40 kV and 40 mA with a step-width of 0.10° 2θ and counting times of 7 s. Rietveld analysis was done using the program Rietan-2000 (Izumi and Ikeda 2000); the single-crystal data for synthetic potassium fluor-richterite (Cameron et al. 1983) were used as the initial parameters, and isotropic displacement factors were used.

FTIR spectra

Samples were prepared for infrared spectroscopy as ~200 mg KBr discs 10 mm in diameter and containing 4-9 mg of fine-grained amphibole. Infrared spectra were recorded in the range 3800~2000 cm^{-1} with a JASCO FTIR-620 spectrometer equipped with a DLATGS detector and a KBr beam splitter. Each sample was scanned 128 times in an evacuated sample-chamber at a nominal resolution of 1 cm^{-1}. After the background was subtracted (as a smoothly curved line [spline]) from the raw data, each spectrum was fitted to component pseudo-Voigt bands, i.e., a Lorentzian peak + Gaussian broadening; this function gives much better analytical results with smaller residuals than either function alone. For spectra obtained in the lattice vibrational range of 1300~400 cm^{-1}, the KBr discs contained about 1 mg of amphibole and were scanned 32 times at a nominal resolution of 4 or 2 cm^{-1}.

TABLE 1. Synthesis conditions for Si-Ge richterites

Run no.	Symbol	Nominal composition	*T* (°C)	*P* (MPa)	Duration (h)
[45]	KGe0Ri	$K(NaCa)Mg_5Si_8O_{22}(OH)_2$	895	745	47.3
[46]	Ge0Ri	$Na(NaCa)Mg_5Si_8O_{22}(OH)_2$	905	727	54.2
[50]	Ge2Ri	$Na(NaCa)Mg_5Si_6Ge_2O_{22}(OH)_2$	866	756	39.5
[51]	Ge4Ri	$Na(NaCa)Mg_5Si_4Ge_4O_{22}(OH)_2$	840	756	39.5
[53]	Ge6Ri	$Na(NaCa)Mg_5Si_2Ge_6O_{22}(OH)_2$	805	720	68.8
[54]	Ge8Ri	$Na(NaCa)Mg_5Ge_8O_{22}(OH)_2$	795	720	68.8

Note: Estimated uncertainties in temperature and pressure are ±5 °C and ±5 MPa, respectively.

RESULTS AND DISCUSSION

Products of synthesis

For almost all experiments for each starting composition along the Si-Ge richterite join, more than 95% amphibole yield was obtained under the experimental conditions used, suggesting a complete solid-solution along the Si-Ge richterite series. Deuteration experiments also achieved up to 95% D exchange, judging from their infrared OH/OD-stretching band intensities. This allowed us to obtain high-quality crystal chemical data using conventional analytical methods, such as X-ray Rietveld refinement and FTIR.

SEM, HRTEM, and AN-TEM

The synthetic amphibole crystals obtained in this study were acicular in shape, being up to 10 μm in length along *c* and <5 μm in diameter (Fig. 1). Very small grains are often present and evenly coat the larger grains. These small grains are presumably amphibole based on their habit, but direct identification of these small grains has not yet been made. With increasing Ge contents the number of fibrous amphibole crystals smaller than 0.5 × 0.5 × 5 μm tends to increase relative to the number of larger acicular crystals.

Examination by HRTEM shows that these synthetic amphiboles are essentially free of chain-multiplicity faults (CMFs).

Semi-quantitative AN-TEM analysis offered general confirmation of the existence of Si-Ge solid solution along the compositional join. Unfortunately, the EDS analyses produced cation totals, calculated on the basis of 8 Si + Ge cations, that were unrealistically low (<<15.0 atoms per formula unit, apfu) for an amphibole structure. The Mg contents for Ge-rich amphiboles were particularly low, suggesting that the EDS software was not able to correctly resolve the overlap in the characteristic X-rays of Mg ($K\alpha$) and Ge ($L\alpha$, $L\beta$). Even if peak overlap corrections can be made, this study suggests that additional problems can arise in the matrix correction scheme for Na-Mg-Ge-rich phases, as discussed in the next section.

Electron microprobe

The electron microprobe analyses of the high-pressure series of amphiboles are listed in Table 2. The energy-overlap problems for the characteristic X-ray lines mentioned above are not so great a problem for WDS analyses where the lines can be separated. However, there is apparently a problem with the ZAF correction scheme for amphiboles with high Ge contents because the total cations, calculated on the basis of 23 O atoms (middle section of Table 2), exceeds the crystal-chemical limit of 16 apfu. This problem is most noticeable for samples Ge4Ri, Ge6Ri, and Ge8Ri. An examination of the individual ZAF terms shows that the A (absorption) term becomes very large for Na and Mg, the two softest characteristic X-rays, as the Ge content increases. Analytical standards having Na and Mg in a Ge-rich matrix would probably remove these large corrections, but such standards are not available at Binghamton University. Based on the FTIR spectra (discussed below), the pure Ge-richterite sample (Ge8Ri) has an almost completely filled A site (virtually no Tr band). Assuming there are no M4-site vacancies, the total cations should in fact

add up to 16.0 on the basis of 23 O atoms. This condition can be met for the pure Ge-richterite sample by reducing the Na_2O and MgO contents by 25 and 20 wt%, respectively. A greater correction seems reasonable for Na compared to Mg because of the slighter softer (longer) characteristic wavelength being used for Na compared to Mg. Applying this correction to the three most Ge-rich samples in proportion to the amount of GeO_2 present in the amphibole (the exact expression is given at the bottom of Table 2), one obtains cation totals within the allowed limit of 16 apfu with total Ge and Si contents in the range of 7.91~8.07 apfu (Table 2). We emphasize that this correction is offered only as a first attempt to compensate for the lack of appropriate Na-Mg-Ge-rich standards; until such standards are available these analyses should not be regarded as definitive.

X-ray Rietveld refinement

In almost all synthetic products, the amphibole yield is more than 95% with minor Si-Ge wollastonite as the only other phase. Indexed XRD data for Ge8Ri are given in Table 3. The evolution of XRD patterns for Ge = 0, 4, and 8 apfu for which Rietveld refinements have been done is shown in Figure 2. Note how the intensity of the 110 reflection around 10° 2θ decreases greatly with Ge substitution. The intensity ratio I_{020}/I_{110} actually reverses for the Ge6Ri and Ge8Ri samples: this intensity reversal is quite rare in amphiboles. Reversals in the reflection angles and/or intensities are observed with increasing Ge for many of the reflections, such as $\bar{1}11$ and 200, the $\bar{3}51$ and $\bar{4}21$, the$\bar{1}71$ and $\bar{3}12$, etc. (Fig. 2). Merging of reflections also occurs with increasing Ge content, such as seen for 221 and $\bar{1}51$, and 061, 002, and $\bar{2}02$ (Fig. 2). Rietveld refinement data, the atomic coordinates, and the calculated bond-lengths and bond-angles are given in Tables 4, 5, and 6. The cell dimensions, atomic coordinates, and bond lengths for synthetic richterite from the study of Della Ventura et al. (1997) are also given in Tables 4, 5, and 6 for comparison.

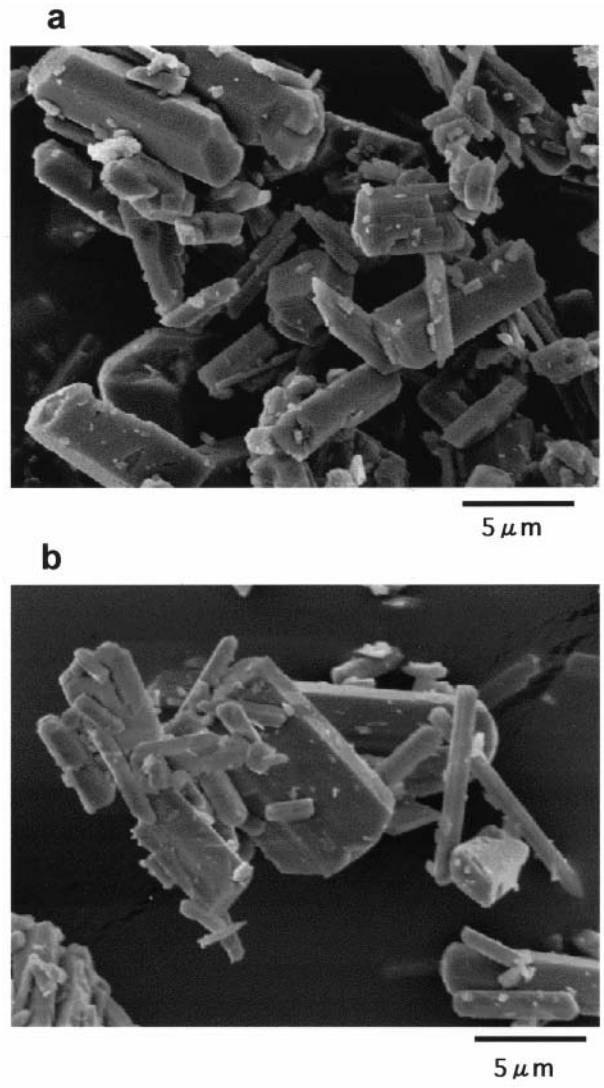

FIGURE 1. SEM images of synthetic (Si,Ge)-richterites. (**a**) [51]Ge4Ri. (**b**) [54]Ge8Ri.

Cell dimensions. The measured cell parameters of the synthetic amphiboles are plotted in Figure 3. The data points show a linear relationship for values from Ge0Ri to Ge8Ri, which is supporting evidence for the presence of a continuous solid-solution series along this join. Cell dimensions for both Na- and K-richterite end-members in this study are quite similar to those reported by Robert et al. (1989), Della Ventura et al. (1993a), Hawthorne et al. (1997), and Della Ventura et al. (1997, 1999).

The T sites. Direct refinement of the Ge and Si occupancy at the T1 and T2 sites was readily accomplished because of the large difference in the X-ray scattering factors of Si and Ge. The refined total Ge contents in Table 4, which were obtained completely independently from any microprobe or AN-TEM results, correspond very closely (within 2σ) to the nominal values. Sample Ge4Ri shows the greatest deviation with an observed 4.13 Ge apfu compared to the expected value of 4.00. With increasing Ge content, there is a marked preference of Ge for the T2 over the T1 site (Fig. 4). This preferential site partitioning is most clearly

TABLE 2. Electron microprobe analysis of the amphiboles synthesized in this study reported as averages of *n* analyses, with uncertainties (1σ) in the last digit shown in parentheses

	Sample					
oxide/ cation	KGe0Ri *n* = 12	Ge0Ri *n* = 12	Ge2Ri *n* = 14	Ge4Ri *n* = 11	Ge6Ri *n* = 9	Ge8Ri *n* = 13
			wt% oxide			
SiO_2	57.0(27)	52.8(89)	41.8(20)	25.9(18)	11.8(50)	0.01(1)
GeO_2	-	-	20.3(14)	39.3(27)	54.1(14)	66.5(49)
MgO	23.4(11)	21.4(34)	23.8(15)	24.4(15)	22.8(54)	21.1(14)
CaO	6.45(22)	5.98(78)	6.10(26)	5.58(26)	5.15(16)	4.67(41)
Na_2O	3.75(21)	6.4(11)	6.53(25)	6.48(47)	6.40(24)	6.03(43)
K_2O	4.93(20)	–	–	–	–	–
Total	95.6(42)	86(14)	98.5(47)	101(6)	100(2)	98.3(70)
			cations per 23 O atoms			
Si	8.06(6)	8.08(5)	6.19(12)	4.09(8)	2.07(8)	0.00(1)
Ge	-	-	1.72(6)	3.56(6)	5.44(6)	7.40(4)
Mg	4.94(9)	4.89(7)	5.26(16)	5.75(12)	5.93(8)	6.10(8)
Ca	0.98(2)	0.99(6)	0.97(3)	0.94(3)	0.96(3)	0.97(3)
Na	1.03(4)	1.91(12)	1.88(10)	1.99(7)	2.17(7)	2.27(9)
K	0.89(3)	–	–	–	–	–
Total	15.89(8)	15.88(9)	16.02(10)	16.34(4)	16.58(4)	16.73(8)
			corrected cations per 23 O atoms*			
Si	–	–	6.31(12)	4.25(8)	2.18(9)	0.00(1)
Ge	–	–	1.76(6)	3.70(6)	5.73(7)	7.92(4)
Mg*	–	–	5.01(15)	5.25(10)	5.23(7)	5.22(8)
Ca	–	–	0.99(3)	0.98(3)	1.02(3)	1.04(3)
Na*	–	–	1.76(10)	1.75(7)	1.82(6)	1.82(7)
Total	–	–	15.82(10)	15.93(4)	15.99(4)	15.99(6)

*MgO and Na_2O were corrected by the expressions MgO(true) = MgO (obs) – 0.20[GeO_2/(GeO_2 + SiO_2)](obs), and Na_2O(true) = Na_2O (obs) – 0.25[GeO_2/(GeO_2 + SiO_2)](obs) before calculating the cations, as discussed in the text.

TABLE 3. Indexed powder pattern for Ge-richterite (Ge8Ri)

hkl	d_{calc} (°)	2Θ*	I_{calc}	*hkl*	d_{calc} (°)	2Θ*	I_{calc}
0 2 0	9.14	9.67	10	$\bar{3}$ 3 2	2.2220	40.57	3
1 1 0	8.721	10.13	2	1 7 1	2.2109	40.78	8
$\underline{1}$ 3 0	5.1930	17.06	5	2 6 1	2.1986	41.02	1
$\bar{1}$ 1 1	5.0278	17.63	29	1 3 2	2.1980	41.03	6
2 0 0	4.9616	17.86	99	$\underline{4}$ 4 0	2.1804	41.38	2
0 4 0	4.5706	19.40	44	1 5 2	2.1718	41.55	1
0 2 1	4.5134	19.65	10	2 0 2	2.0764	43.55	18
$\underline{1}$ 1 1	4.0496	21.93	15	$\underline{2}$ 8 0	2.0757	43.57	13
$\bar{1}$ 3 1	3.9686	22.38	54	$\underline{5}$ 1 1	2.0394	44.38	1
1 3 1	3.4317	25.94	64	$\underline{3}$ 7 1	2.0287	44.63	11
0 4 1	3.4302	25.95	1	3 5 2	1.9983	45.35	1
2 4 0	3.3617	26.49	65	1 9 0	1.9901	45.54	1
$\underline{3}$ 1 0	3.2549	27.38	82	4 2 1	1.9826	45.72	10
$\bar{3}$ 1 1	3.1721	28.11	11	$\underline{5}$ 1 0	1.9731	45.96	23
$\underline{2}$ 2 1	2.9997	29.76	51	$\underline{5}$ 3 1	1.9449	46.66	2
1 5 1	2.9966	29.79	72	$\underline{4}$ 4 2	1.9133	47.48	10
$\underline{3}$ 3 0	2.9071	30.73	27	1 9 1	1.8935	48.01	17
3 3 1	2.8477	31.39	50	2 4 2	1.8904	48.09	2
$\underline{1}$ 5 1	2.7443	32.60	100	$\underline{5}$ 3 0	1.8871	48.18	11
1 1 2	2.6706	33.53	3	1 7 2	1.8771	48.45	4
$\underline{0}$ 6 1	2.6277	34.09	63	4 4 1	1.8559	49.04	1
2 0 2	2.6147	34.27	82	$\underline{2}$ 8 1	1.8549	49.07	1
$\underline{0}$ 0 2	2.5951	34.53	35	5 1 2	1.8311	49.75	4
$\underline{4}$ 0 1	2.5257	35.51	1	0 10 0	1.8282	49.84	5
$\bar{2}$ 2 2	2.5139	35.69	1	1 9 1	1.8248	49.94	6
4 0 0	2.4808	36.18	10	$\underline{3}$ 1 2	1.8044	50.54	14
$\underline{3}$ 1 1	2.4720	36.31	1	$\underline{5}$ 5 1	1.7896	50.99	8
$\underline{2}$ 6 1	2.4691	36.36	7	$\underline{1}$ 1 3	1.7814	51.24	1
1 3 2	2.4682	36.37	3	_5 3 2	1.7617	51.86	1
$\underline{3}$ 5 0	2.4530	36.60	4	2 2 3	1.7611	51.87	1
$\underline{4}$ 2 1	2.4345	36.89	18	1 7 2	1.7497	52.24	2
$\underline{3}$ 5 1	2.4170	37.17	83	3 3 2	1.7380	52.62	7
$\bar{3}$ 1 2	2.3661	38.00	10	3 9 0	1.7310	52.85	2
$\underline{1}$ 1 2	2.3373	38.48	10	0 10 1	1.7244	53.06	2
1 7 1	2.3366	38.50	29	$\underline{2}$ 8 2	1.7207	53.19	12
0 8 0	2.2853	39.40	6	$\underline{3}$ 9 1	1.7182	53.27	9
0 4 2	2.2567	39.92	8	1 3 3	1.7174	53.30	7

* 2Θ calculated for Cu$K\alpha$1 radiation (1.54056 Å).

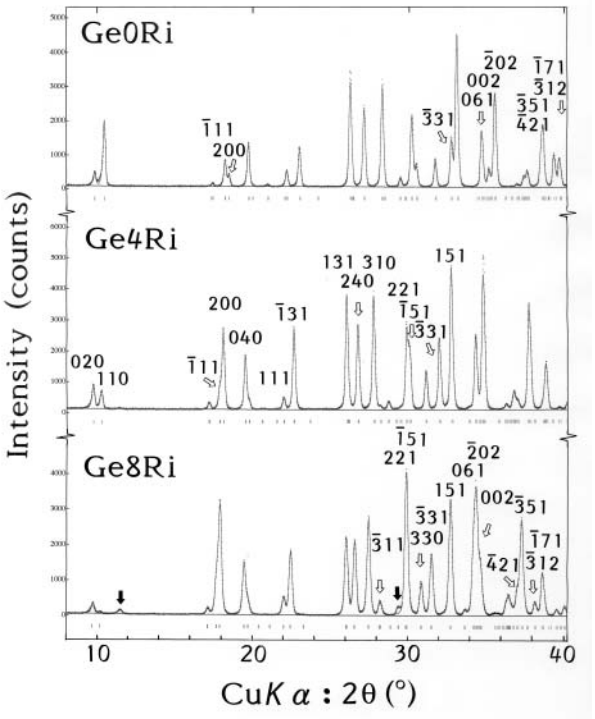

FIGURE 2. Observed (crosses), calculated (line) powder XRD patterns for several synthetic (Si,Ge)-richterites. The white arrows refer to Miller indices of Bragg reflections while the solid arrows indicate non-amphibole phase(s).

seen for sample Ge2Ri, where there is about twice as much Ge at the T2 compared to the T1 site (Table 4). Despite the preference of Ge for the T2 site, there appears to be a linear increase in the mean <T1-O> and <T2-O> bond distances with increasing Ge content across the join (Fig. 5), with the <T2-O> distance always being larger than <T1-O>.

TABLE 4. Rietveld refinement of synthetic Si-Ge richterites (monoclinic, *C2/m*)

Sample	Mg(100)*	KGe0Ri	Ge0Ri	Ge2Ri	Ge4Ri	Ge6Ri	Ge8Ri
Collecting conditions							
2θ scan range (°)	9–100	8–120	8–120	8–120	8–120	8–120	8–120
Step interval (°)	0.1	0.1	0.1	0.1	0.1	0.1	0.1
Integration time (s)	5	7	7	7	7	7	7
*R*wp(%)	12.93	7.95	10.05	7.73	9.11	6.55	8.88
*R*p(%)	9.99	5.69	7.70	5.82	7.05	4.85	6.57
*R*e(%)	–	4.84	4.64	4.16	4.01	3.89	3.60
S	–	1.6443	2.1657	1.8606	2.2718	1.6843	2.4678
Durbin-Watson *d*	1.44	1.43	1.24	1.05	1.18	1.08	1.16
Agreement indices							
a (Å)	9.9076(6)	10.0439(5)	9.9032(6)	10.0144(6)	10.1237(7)	10.2255(9)	10.3244(8)
b (Å)	17.988(1)	17.9883(7)	17.9885(9)	18.071(1)	18.147(1)	18.2144(1)	18.282(1)
c (Å)	5.2706(4)	5.2708(2)	5.2692(3)	5.3058(3)	5.3386(4)	5.3683(5)	5.3994(4)
β (°)	104.252(4)	104.803(2)	104.250(3)	104.625(3)	105.067(4)	105.555(4)	106.015(4)
V (Å^3)	910.41	920.69(7)	909.79(9)	929.1(1)	947.1(1)	963.2(1)	979.6(1)
*a*sinβ(Å)	–	9.7105	9.5985	9.6899	9.7757	9.8510	9.9237
Site-occupancies, atoms per formula unit							
T1 Si	4.000	4.000	4.000	3.31(3)	2.32(4)	1.24(4)	-
Ge	-	-	-	0.69(3)	1.68(4)	2.76(4)	4.000
T2 Si	4.000	4.000	4.000	2.62(3)	1.56(4)	0.68(4)	-
Ge	-	-	-	1.38(3)	2.45(4)	3.32(4)	4.000
Sum of T sites, Si	8.000	8.000	8.000	5.93(4)	3.88(6)	1.92(6)	-
Sum of T sites, Ge	-	-	-	2.07(4)	4.13(6)	6.08(6)	8.000
M4 Ca	1.05(1)	1.02(4)	0.98(4)	0.90(4)	0.98(6)	0.88(3)	0.84(6)
Na	0.95(1)	0.98(4)	1.02(4)	1.10(4)	1.02(6)	1.12(3)	1.16(6)
A Na	0.95(1)	K=0.954(8)	0.85(2)	0.87(4)	0.89(2)	0.91(2)	0.92(3)

* Della Ventura et al. (1997).

Rotation angles of the double chains. With increasing Ge for Si substitution, the O5-O6-O5 and the T-O-T angles decrease (Fig. 5) to compensate for the increasing misfit between the lateral dimensions of the octahedral strip and the tetrahedral double chain. This means that the tetrahedral rotation increases as the average radius of the tetrahedrally coordinated cation increases. On the other hand, the size of the Mg-octahedra do not change (Table 6, Fig. 5).

The M1~M4 and A sites. The variations of the mean bond lengths for the M1~M4 and A sites, labeled <M1~M4-O> and <A-O>, respectively, are very small and do not show any correlation with the tetrahedral Ge contents (Fig.

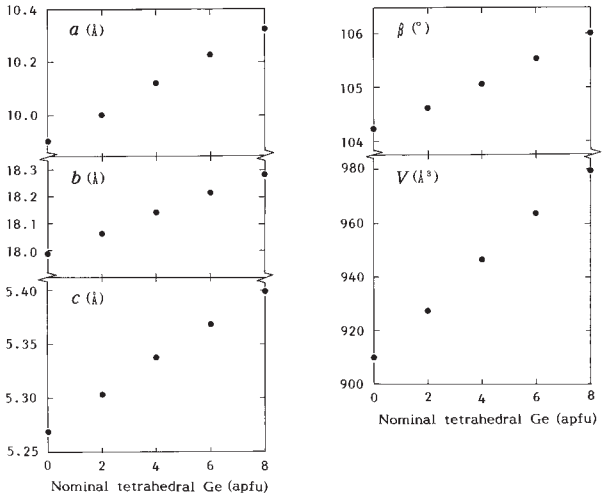

FIGURE 3. Lattice parameters *a*, *b*, *c*, β, and cell volume *V* of amphiboles synthesized along the (Si,Ge)-richterite join. Standard deviations (1σ) are within the symbols.

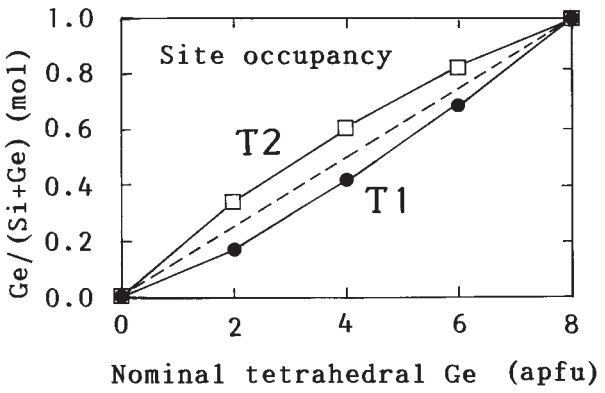

FIGURE 4. Molar ratio of Ge/(Ge + Si) at the T1 and T2 tetrahedral sites as a function of the nominal total Ge content in atoms per formula unit (apfu). Dashed line shows the 1:1 correlation.

5); this is because only Mg occupies the M1~M3 sites, and the populations of Ca and Na at the M4 sites are nearly constant with Ca/Na = 1. However, the M4-O6 distances become longer than those for M4-O5 at a bulk composition of about Ge = 3 apfu, and a reverse relationship exists between the A-O6 and A-O5 distances; this agrees with the observed increase in the rotation of the tetrahedral chains to compensate for the misfit between the octahedral and tetrahedral sites. Both the electron microprobe analysis (Table 2) and the Rietveld refinements (Table 4) of the Ge-free richterite sample Ge0Ri indicate a slight deficiency of Na at the A site (0.85–0.90 apfu). This agrees with the presence of A-site-vacant, so-called tremolite bands, in the OH-stretching range of the FTIR spectra, as discussed below, and with previous studies of synthetic richterite (e.g., Gottshalk and Andrut 1998; Della Ventura et al. 1999). In view of the difficulties encountered in this study with the AN-TEM and electron microprobe analysis of the Ge-bearing amphiboles, we suggest that Na occupancy at the A site for the entire amphibole series may be more accurately determined using the values refined by the Rietveld method or calculated from the relative intensities of the infrared OH-stretching bands.

FTIR

OH/OD-stretching bands. Two kinds of infrared OH/OD-stretching bands, attributed here to the (MgMgMg)-OH/OD-^{A}Na and (MgMgMg)-OH/OD-$^{A}\square$ configurations, were observed in the Si-Ge richterite series (Figs. 6a and 6b). The former bands appear at higher frequencies and are referred to as the richterite bands (designated here as Ri bands, modified slightly from Hawthorne et al. 1997), while the latter appear at lower frequencies and are referred to as the tremolite bands (Tr bands, as above). Frequency ratios ν_{OH}/ν_{OD} are 1.355~1.357, which are very close to the theoretical value predicted for simple harmonic oscillation (= 1.374, Langer and Lattard 1980). With increasing Ge contents the frequencies of both types of bands for the Na-bearing richterites decrease linearly (Table 7). The band width of the Ri bands, measured as the full-width at half-maximum height (FWHM), is nearly twice as wide as that of the Tr bands, mainly because of the positional disorder of Na at the A site (Hawthorne et al. 1997) but probably also because of Ca^{2+}, Mg^{2+}, and Na^{+} cation disorder at the M4-site (Melzer et al. 2000). A comparison of the OH/OD-stretching bands for KGe0Ri and Ge0Ri shows that the frequency of the Tr band of Ge0Ri is higher by 3.5 cm^{-1} for the OH-form and by 2.6 cm^{-1} for the OD-form relative to those in KGe0Ri. This is attributed to the presence of a larger vacant A site in KGe0Ri than in Ge0Ri, which is caused by the surrounding occupied A-site ion being larger in KGeORi (=K) than in Ge0Ri (= Na). As a result, the average <A-O> distance is slightly larger (Table 6) and the O3-O7 distances slightly shorter (by about 0.1 Å) in KGe0Ri than in Ge0Ri. Della Ventura et al. (1999) have stressed the influence that the O7 atom exerts on the OH-stretching vibration of A-site-occupied amphiboles. The result is a tendency toward hydrogen bond formation along the O3-H/D···O7 direction, making the O3-H/D interaction slightly weaker in KGe0Ri than in Ge0Ri.

With increasing Ge contents, the intensity of the Tr bands, or the (MgMgMg)-OH/OD-$^{A}\square$ stretching band, decreases and the band almost disappears at the Ge8Ri end-member. As mentioned previously, the FTIR spectra in the OH-stretching region may provide the most reliable assessment of the Na content at the A sites. Using the technique described by Hawthorne et al. (1997) and further refined by Melzer et al. (2000), the mole fraction of the A-site vacancy content (X^{Tr}) can be calculated from the expression $X^{Tr} = R/[k + R(1–k)]$, where R is the ratio of the Tr band (I^{Tr}) and Ri band (I^{Ri}) intensities [$R = I^{Tr}/(I^{Tr} + I^{Ri})$] and k is a constant which corrects the intensities of the Tr and Ri bands for differences in molar absorptivities between the bands. Hawthorne et al. (1997) derived a value of 2.2 for k for the join K-richterite–tremolite, while Melzer et al. (2000) derived a value of 1.68 from their study of the K-richterite–richterite–tremolite ternary system. Melzer et al. (2000) also proposed that the molar absorbance of the OH-stretching vibrations depends only on the energy of the vibration and not on the composition of the amphibole. Assuming a linear relationship between the extinction coefficient (ε) and the wavenumber (ν) of the Ri band, Melzer et al. (2000) proposed the relationship (from their corrected Eq. 10) $1/k = 1 – 0.00703(\nu – 3674.6)$. Using the band intensities from Table 7 and the expression for k from Melzer et al. (2000), we obtain the values of X^{Tr} and X^{Ri} (= $1– X^{Tr}$) shown in Table 8. There is excellent agreement between the FTIR and Rietveld-refined K contents for the K-rich-

TABLE 5. Atomic parameters for synthetic Si-Ge richterites

Atom		Mg(100)*	KGe0Ri	Ge0Ri	Ge2Ri	Ge4Ri	Ge6Ri	Ge8Ri
	x	0.2808(10)	0.2750(4)	0.2791(7)	0.2805(5)	0.2803(6)	0.2796(4)	0.2795(4)
T1	*y*	0.0853(4)	0.0851(2)	0.0844(3)	0.0842(2)	0.0850(2)	0.0853(1)	0.0856(2)
	z	0.2977(21)	0.3018(9)	0.295(1)	0.299(1)	0.304(1)	0.3064(7)	0.3090(8)
	x	0.2847(12)	0.2839(5)	0.2858(7)	0.2855(5)	0.2856(5)	0.2861(4)	0.2871(4)
T2	*y*	0.1697(4)	0.1711(2)	0.1704(3)	0.1721(2)	0.1731(2)	0.1739(1)	0.1745(2)
	z	0.7973(22)	0.8037(9)	0.799(1)	0.8045(8)	0.8087(9)	0.8122(7)	0.8147(8)
	x	0	0	0	0	0	0	0
M1	*y*	0.0892(8)	0.0900(4)	0.0886(4)	0.0878(4)	0.0882(6)	0.0868(5)	0.0867(7)
	z	½	½	½	½	½	½	½
	x	0	0	0	0	0	0	0
M2	*y*	0.1772(7)	0.1798(4)	0.1785(5)	0.1785(5)	0.1783(7)	0.1776(6)	0.1781(8)
	z	0	0	0	0	0	0	0
	x	0	0	0	0	0	0	0
M3	*y*	0	0	0	0	0	0	0
	z	0	0	0	0	0	0	0
	x	0	0	0	0	0	0	0
M4	y	0.2751(7)	0.2777(3)	0.2779(4)	0.2782(4)	0.2773(5)	0.2758(5)	0.2743(6)
	z	½	½	½	½	½	½	½
	x	0	0	0	0	0	0	0
A	*y*	0.4791(22)	½	½	½	½	½	½
	z	0	0	0	0	0	0	0
	x	0.1165(18)	0.1132(8)	0.120(1)	0.116(1)	0.113(2)	0.108(2)	0.108(2)
O1	*y*	0.0870(9)	0.0873(4)	0.0861(5)	0.0859(5)	0.0839(7)	0.0848(5)	0.0843(7)
	z	0.2234(33)	0.219(2)	0.219(2)	0.221(2)	0.217(3)	0.221(2)	0.216(3)
	x	0.1079(20)	0.1177(9)	0.117(1)	0.114(1)	0.113(2)	0.114(1)	0.112(2)
O2	*y*	0.1695(9)	0.1722(4)	0.1700(5)	0.1696(6)	0.1702(8)	0.1698(7)	0.1703(9)
	z	0.7169(35)	0.722(2)	0.723(2)	0.727(2)	0.726(3)	0.727(2)	0.732(3)
	x	0.1066(19)	0.111(1)	0.109(1)	0.107(1)	0.106(2)	0.107(2)	0.103(2)
O3	*y*	0	0	0	0	0	0	0
	z	0.7120(48)	0.721(2)	0.718(3)	0.718(3)	0.725(4)	0.719(4)	0.716(5)
	x	0.3538(17)	0.359(1)	0.357(1)	0.357(1)	0.355(2)	0.363(2)	0.361(2)
O4	*y*	0.2493(8)	0.2468(4)	0.2464(5)	0.2475(5)	0.2495(7)	0.2503(6)	0.2518(8)
	z	0.7796(43)	0.796(2)	0.797(2)	0.791(3)	0.790(4)	0.781(3)	0.779(4)
	x	0.3433(21)	0.341(1)	0.348(1)	0.346(1)	0.346(2)	0.349(1)	0.351(2)
O5	*y*	0.1296(8)	0.1282(4)	0.1298(5)	0.1323(5)	0.1365(7)	0.1388(6)	0.1417(8)
	z	0.0863(39)	0.098(2)	0.095(2)	0.109(3)	0.121(4)	0.135(3)	0.148(4)
	x	0.3389(19)	0.340(1)	0.341(1)	0.341(1)	0.342(2)	0.345(1)	0.344(2)
O6	*y*	0.1122(9)	0.1160(4)	0.1161(5)	0.1134(5)	0.1099(7)	0.1049(6)	0.1039(7)
	z	0.5966(37)	0.595(2)	0.589(2)	0.601(3)	0.624(4)	0.629(4)	0.631(4)
	x	0.3379(25)	0.332(1)	0.339(1)	0.339(2)	0.339(2)	0.340(2)	0.344(2)
O7	*y*	0	0	0	0	0	0	0
	z	0.3025(50)	0.301(3)	0.280(3)	0.268(3)	0.262(5)	0.258(4)	0.246(5)

Note: Isotropic temperature factors from Cameron et al. (1983); T1 = 0.51, T2 = 0.50, M1 = 0.47, M2 = 0.61, M3 = 0.42, M4 = 1.58, A = 2.68, O1 = 0.69, O2 = 0.64, O3 = 0.64, O4 = 0.96, O5 = 0.86, O6 = 0.84, O7 = 0.93.
* Della Ventura et al. (1997)

terite sample (KGe0Ri). There is general agreement between the FTIR and Rietveld refinements for the remaining samples, such that both methods indicate a deficiency of Na in amphiboles that are nominally A-site filled; however, the FTIR spectra indicate uniformly higher Na contents.

Except for Ge8Ri, the FWHM values for the OH-stretching Ri bands are very similar and range from 18~20 cm^{-1}. A linear frequency decrease with increasing Ge substitution without band-width broadening implies that the electronic environment around the proton of the O3-H hydroxyl group varies rather continuously. It is recognized that this behavior is unusual and does not readily conform to existing studies of amphibole infrared spectra. Accordingly, we offer two possible explanations. First, as the electronegativity of Ge is greater than that of Si, the electrons of the O atoms coordinated to tetrahedral Ge polarize to the surrounding cations to a greater extent than the O atoms coordinated to Si. This implies that the degree of hydrogen bonding increases. Second, with increasing Ge substitution the height of the tetrahedra becomes larger and thus the (O3)H-Na distance becomes longer; this will cause a decrease in the repulsive force between the proton and Na atom and thus contribute to the downward frequency shift of the OH/OD bands. Both of these effects will act to cause a downward shift in the frequency (wavenumber) of the Ri bands, though only the former process could occur in the Ge analogue of talc as discussed below. It is important to stress that the change in the OH-stretching frequency appears to be continuous along this series without the presence of any readily identifiable fine structure that would result from short-range ordering of the tetrahedral cations.

Lattice vibrational bands. The FTIR spectra in the lattice-vibration range of 1300~400 cm^{-1} are shown in Figure 7 for the hydroxyl (solid curve) and deuterated (dashed curve) samples. There is excellent agreement between the richterite spectrum obtained in this study (Ge0Ri) and that reported by Andrut et al. (2000). The spectra for both richterite and K-richterite (KGe0Ri) are quite similar except for minor differences in some Si-O stretching bands at 1125~1025 cm^{-1}.

A look at the frequencies of the infrared bands in the lattice-vibration region across the Si-Ge richterite series shows that the spectra may be divided into three regions (Fig. 7) corresponding to the groupings of lattice vibrations that have been observed in earlier studies (e.g., Lazarev 1972, Ch. 3; Farmer 1975). In region 1, there are 8 to 7 strong to medium-strong Si-O or Ge-O stretching bands. These occur in the range of 1300~800 cm^{-1} for the Si end-member and in the range of 920~700 cm^{-1} for the Ge end-member. In region 2, there are 6 to 4 medium, weak, very weak, and shoulder bands in the range of 800~570 cm^{-1} for the Si end-member and in the range of 700~505 cm^{-1} for the Ge end-member. At least three bands ascribed to chain deformations plus an OH librational band appear in this region. In region 3, M-O (M = Mg, Na, Ca, Si, and Ge) deformation bands occur below 570

TABLE 6. Selected bond-lengths (Å) and bond angles (°) for synthetic Si-Ge richterites

Sample	Mg(100)*	KGe0Ri	Ge0Ri	Ge2Ri	Ge4Ri	Ge6Ri	Ge8Ri
Selected bond-lengths (Å)							
T1-O1	1.577(19)	1.572(8)	1.531(10)	1.593(10)	1.639(15)	1.690(14)	1.714(17)
T1-O5	1.611(23)	1.601(8)	1.615(10)	1.589(12)	1.612(15)	1.630(13)	1.645(15)
T1-O6	1.611(20)	1.613(10)	1.624(12)	1.652(14)	1.724(18)	1.721(16)	1.715(20)
T1-O7	1.633(11)	1.635(5)	1.640(6)	1.653(6)	1.688(8)	1.719(7)	1.763(11)
<T1-O>	1.608(9)	1.605	1.603	1.622	1.666	1.690	1.709
T2-O2	1.696(22)	1.614(8)	1.619(10)	1.660(10)	1.689(14)	1.701(13)	1.728(16)
T2-O4	1.600(17)	1.561(7)	1.539(9)	1.549(10)	1.567(14)	1.627(13)	1.654(17)
T2-O5	1.658(21)	1.696(10)	1.693(13)	1.729(14)	1.752(19)	1.796(17)	1.833(19)
T2-O6	1.661(22)	1.682(9)	1.668(10)	1.704(12)	1.703(16)	1.796(13)	1.824(15)
<T2-O>	1.654(9)	1.638	1.630	1.661	1.678	1.730	1.760
M1-O1 (×2)	2.071(19)	2.086(8)	2.113(10)	2.102(11)	2.115(16)	2.086(14)	2.115(18)
M1-O2 (×2)	1.981(19)	2.061(9)	2.049(11)	2.059(12)	2.065(16)	2.089(14)	2.111(19)
M1-O3 (×2)	2.088(16)	2.136(9)	2.101(10)	2.089(11)	2.115(16)	2.096(14)	2.090(17)
<M1-O>	2.047(10)	2.094	2.088	2.083	2.098	2.090	2.105
M2-O1 (×2)	2.164(18)	2.173(8)	2.196(10)	2.198(11)	2.212(15)	2.187(12)	2.199(15)
M2-O2 (×2)	2.042(21)	2.108(9)	2.083(10)	2.067(11)	2.080(16)	2.106(15)	2.104(19)
M2-O4 (×2)	2.090(17)	2.035(10)	2.057(12)	2.064(14)	2.068(20)	2.049(17)	2.032(22)
<M2-O>	2.099(11)	2.105	2.112	2.110	2.120	2.114	2.112
M3-O1 (×4)	2.121(15)	2.103(7)	2.112(9)	2.107(9)	2.067(12)	2.077(10)	2.061(13)
M3-O3 (×2)	2.051(25)	2.061(11)	2.041(13)	2.045(15)	2.028(20)	2.087(17)	2.092(25)
<M3-O>	2.098(8)	2.089	2.088	2.086	2.054	2.080	2.071
M4-O2 (×2)	2.333(19)	2.380(8)	2.412(10)	2.429(10)	2.414(14)	2.410(12)	2.395(16)
M4-O4 (×2)	2.346(22)	2.401(9)	2.397(12)	2.400(13)	2.445(18)	2.370(15)	2.391(23)
M4-O6 (×2)	2.708(20)	2.627(8)	2.588(11)	2.662(11)	2.782(14)	2.881(11)	2.929(15)
$^{[VI]}$<M4-O>	-	2.469	2.466	2.497	2.547	2.554	2.572
M4-O5 (×2)	2.907(18)	2.858(10)	2.828(12)	2.774(13)	2.706(18)	2.651(14)	2.589(18)
$^{[VIII]}$<M4-O>	2.573(10)	2.567	2.556	2.566	2.587	2.578	2.576
A-O5 (×4)	-	2.924(7)	2.885(10)	2.979(9)	3.082(13)	3.147(12)	3.241(16)
A-O6 (×4)	-	3.123(9)	3.137(11)	3.082(11)	2.982(16)	2.904(13)	2.901(17)
A-O7 (×2)	-	2.595(12)	2.425(14)	2.402(16)	2.408(22)	2.409(17)	2.367(25)
<A-O>	-	2.938	2.894	2.905	2.907	2.902	2.836
Selected bond-angles (°)							
T1-O5-T2	-	137.0(7)	134.5(9)	135.8(9)	134.2(11)	131.3(9)	129.3(12)
T1-O6-T2	-	135.2(6)	136.8(8)	135.6(8)	131.4(10)	126.7(8)	126.5(11)
T1-O7-T1	-	139.0(8)	135.6(10)	134.0(10)	132.0(13)	129.5(10)	125.2(15)
O5-O6-O5	-	170.5(4)	168.9(5)	165.2(5)	159.5(7)	154.0(5)	151.0(7)

* Della Ventura et al. (1997).

cm^{-1} in Si-richterite and below 500 cm^{-1} in Ge-richterite.

Si/Ge-O stretching (Region 1). Because of the greater mass of Ge and the longer bond distances (weaker bond strengths), the Ge-O stretching bands shift downward in frequency as expected. The observed frequency ratios of corresponding bands range between 1.23 and 1.27. In addition to this downward shift there is a distinct reduction in the absorption range of the bands assigned to region 1, such that the Si-O stretching bands appear over a range of about 350~400 cm^{-1} while the Ge-O stretching bands appear over a range of 200~250 cm^{-1}, or about half of the width. Deuteration does not have any affect on the bands in this region.

Si/Ge-O chain deformation plus OH libration (Region 2). The medium-strong band at about 740 cm^{-1} in KGe0Ri and Ge0Ri is assigned to Si-O-Si deformation, while the 670 cm^{-1} band is assigned to O-Si-O deformation (Lazarev 1972; Gillet et al. 1989; Ishida 1990) (Fig. 7). These bands also shift downward with increasing Ge content, and the ranges over which these absorption bands occur become narrower: the Si-O chain deformation bands occur over a range of about 120 cm^{-1} while the Si·Ge-O and Ge·Ge-O deformations occur over a range of about 70 cm^{-1}. An OH libration band is clearly identifiable in the Si and Ge end-members because these bands disappear with deuteration. In KGe0Ri and Ge0Ri the OH libration occurs as a broad and weak band centered at about 600 cm^{-1}, while in Ge8Ri it occurs at 650 cm^{-1}. With increasing Ge substitutions, the OH libration band shifts upward and, in the spectra of the intermediate compositions, overlaps with Si/Ge-O chain deformation bands. Thus the downward shift in the OH-stretching bands with increasing Ge content is opposite to that of the libration bands. This type of inverse behavior of the shifts of the OH-stretching and OH-libration bands has been observed in other studies (e.g., Shirozu and Ishida 1982; Ishida 1990) and is consistent with the hypothesis that increased hydrogen bonding occurs in Ge-richterite. That is, increased hydrogen bonding will shift the OH-stretching vibration to lower frequencies (e.g., Libowitzky 1999) and could dampen or restrict the oscillations of the OH group around its center of mass to higher frequencies.

The strong downward shift of the bands in regions 1 and 2 caused by the substitution of Ge for Si stands in sharp contrast to the very limited effect that substitutions at the M4 and A site have on these bands as reported by Andrut et al. (2000). Andrut et al. (2000) showed that substitutions of ^{M4}Sr = ^{M4}Ca in tremolite and ^{A}Na + ^{M4}Na = $^{A}\square$ + ^{M4}Ca along the tremolite-richterite join cause very little change in the band positions in the mid-infrared range of 1300–600 cm^{-1}. They did note an overall reduction in band intensities and an increase in band widths toward the richterite end-member. A comparison of the results presented in this study with those of Andrut et al. (2000) provides confirmation that the bands in regions 1 and 2 are indeed attributed to Si-O stretching and Si-O-Si deformation vibrations, and that these vibrations are largely isolated from the effects of cation substitutions at the M4 and A sites. Andrut et al. (2000) suggested that OH-libration bands might occur in the 850-600 cm^{-1} range for richterite but did not test this hypothesis. The deuteration experiments performed in this study confirm that there is one, but only one, OH-libration band in richterite in this range which is centered at 600 cm^{-1}.

M-O deformation (Region 3). With increasing Ge substitution, the frequencies of these bands shift downward and may shift below the frequency range of the instrument for the most Ge-rich samples. The medium-strength but well-defined band at 550 cm^{-1} for the silicate richterites (KGe0Ri and Ge0Ri) appears to shift downward, merges with lower-frequency bands at intermediate compositions, and then emerges as a medium-strong and well-defined band at 493 cm^{-1} in pure Ge-richterite (Ge8Ri) for a net downward shift of ~70 cm^{-1}. This band occurs at about the frequency expected for octahedral Mg-O stretching vibrations (e.g., Farmer 1975), but it cannot be solely related to Mg-O vibrations because the average M-O distances do not vary significantly across this join (Table 6, Fig. 5). This vibration probably involves some Mg-O-Si/Ge linkage because the frequency shifts by a factor of

TABLE 7. OH/OD-stretching spectra of Si-Ge richterites

Band*	Parameter	Sample					
		KGe0Ri	Ge0Ri	Ge2Ri	Ge4Ri	Ge6Ri	Ge8Ri
OH-form							
Ri band	Position	3732.3	3729.5	3718.3	3706.2	3697.2	3688.7
	Width	16.6	18.1	18.8	19.7	18.2	14.8
	Intensity	0.905	0.882	0.929	0.937	0.976	0.998
	G/(G + L)†	0.872	0.872	1.000	0.911	0.939	0.875
Tr band	Position	3670.6	3674.1	3667.5	3659.8	3650.8	3643.9
	Width	10.8	9.89	10.9	12.4	11.3	9.3
	Intensity	0.096	0.118	0.071	0.063	0.024	0.002
	G/(G + L)	1.000	1.000	1.000	0.066	0.049	1.000

* Ri band = Higher-frequency bands ascribed to M1M1M3-OH/OD-A (A = A-site alkali ions), Tr band = Lower-frequency bands ascribed to M1M1M3-OH/OD-□ (□ = vacant A site)
† Ratio of the Gaussian (G) and Lorentzian (L) components

TABLE 7. – *continued*

Band*	Parameter	Sample					
		[835]KGe0	[836]Ge0	[838]Ge2	[837]Ge4	[847]Ge6	[846]Ge8
OD-form							
Ri band	Position	2751.3	2749.6	2741.4	2733.0	2726.0	2719.7
	νOH/νOD	1.357	1.356	1.356	1.356	1.356	1.356
	Width	11.5	12.8	13.7	14.3	13.2	10.6
	Intensity	0.915	0.889	0.877	0.872	0.96	0.987
	G/(G + L)	0.928	0.955	0.811	0.811	1.000	1.000
Tr band	Position	2707.4	2710.0	2705.5	2700.3	2694.2	2687.3
	νOH/νOD	1.356	1.356	1.356	1.355	1.355	1.356
	Width	6.8	6.5	8.2	13.2	10.5	7.3
	Intensity	0.085	0.111	0.123	0.128	0.040	0.013
	G/(G + L)	0.817	0.890	0.234	0.000	0.000	0.000

only 1.11 and not by the factor of 1.23~1.27 that is observed for other Ge-O vibrations in regions 1 and 2. The remaining bands below 550 cm^{-1} in the Si-richterites are apparently a combination of OH librations and Mg-O and Si/Ge-O bending and deformation bands as indicated by a general downward shift in these bands. Deuteration produces noticeable changes to some of the band structure in region 3, such as the appearance of a sharp and distinct band at ~450 cm^{-1} in KGe0Ri and Ge0Ri that appears to shift upward to ~470 cm^{-1} in Ge4Ri and possibly merges with the 490 cm^{-1} peak in Ge8Ri. These bands are attributed to OD librations. Unfortunately the broad and overlapping nature of the bands in this region make it hard to make any more specific as-

TABLE 8. Mole fraction of A-site vacant (X^{Tr}) and A-site-filled (X^{Ri}) components in amphibole, calculated from FTIR spectra

Sample	Ri band (cm^{-1})	R*	k†	X^{Tr}	X^{Ri}	obs§
KGeORi	3732	0.096	1.68	0.06	0.94	K = 0.95(1)
GeORi	3730	0.118	1.64	0.08	0.92	0.85(2)
Ge2Ri	3718	0.071	1.60	0.05	0.95	0.87(4)
Ge4Ri	3706	0.063	1.28	0.05	0.95	0.89(2)
Ge6Ri	3697	0.024	1.19	0.02	0.98	0.91(2)
Ge8Ri	3689	0.002	1.11	0.002	0.998	0.92(3)

* R = relative intensities of the Tr and Ri bands, defined as $I^{Tr}/(I^{Tr} + I^{Ri})$.
† k = term related to the differences in the molar absorptivity of the Tr and Ri bands (Hawthorne et al. 1997), defined as a function of the Ri band wavenumber by Melzer et al. (2000).
§ Observed Na (or K) content (apfu) at the A site from Rietveld refinements (Table 3).

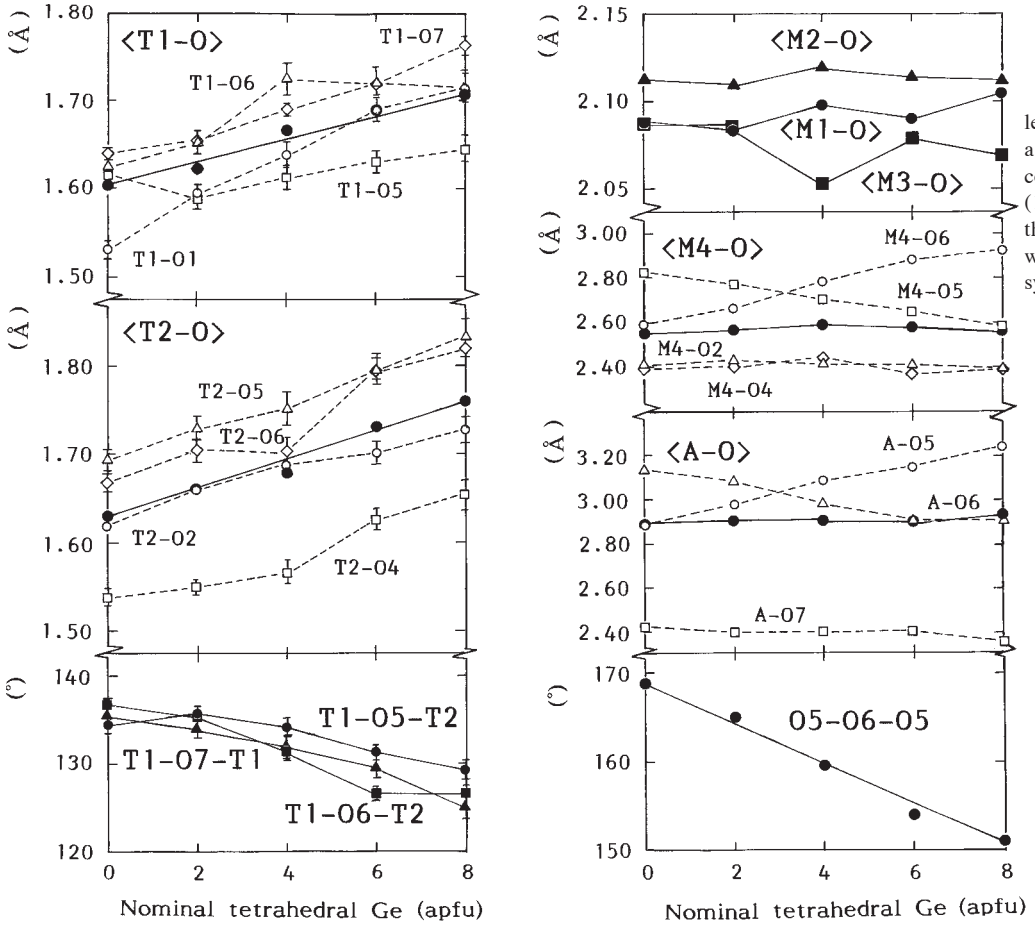

FIGURE 5. Bond-lengths and angles as a function of Si-Ge content. Uncertainties (1σ) are shown by the error bars or are within the size of the symbols.

signments in this region, particularly for a mineral as chemically complex as richterite.

Comparison with other Ge-analogue phases

Although we do not know of other studies involving Ge-rich amphiboles, the earlier studies of Ge-analogues of tri-octahedral layered silicates are relevant to this study because the amphibole double chain can be thought of as one unit of a continuous tetrahedral sheet and because the local environment around the OH group in richterite is the same as that in tri-octahedral layered silicates. Substitution of Ge for Si produced very similar effects in the infrared lattice vibration region of the Ge-analogue of phlogopite [$KMg_3(AlGe_3)O_{10}(OH)_2$] (Jenkins 1989) as were produced for Ge-richterite in this study. Namely, the complete substitution of Ge for Si produces a very noticeable downward shift in the major bands centered at about 1000 cm^{-1}, 700 cm^{-1}, and at 500 cm^{-1}, supporting the assignment of these bands to Si-O stretching, Si-O-Si deformation, and Si-O bending or linked Si-O-Mg vibrations, respectively. The extent of the shift in richterite is greater (factor of 1.24~1.27) than in phlogopite (factor of 1.19), at least for the Si-O stretching and Si-O-Si deformation bands, indicating that tetrahedral cations in a double-chain configuration vibrate at a lower frequency than tetrahedral cations interconnected in a two-dimensional sheet. What this study shows for amphiboles, to the extent that these broad and overlapping bands can be resolved, is (1) there is a continuous shift in the lattice vibrations with substitution of Ge for Si and (2) the Ge-O stretching vibrations of the Ge-analogue phase occur at well-defined energies as indicated by the narrower range over which the absorption bands occur.

Comparing this study to the relatively recent work on Ge-substituted talc by Martin et al. (1996), one can identify two similarities and one distinct difference between the FTIR spectra in the OH-stretching region. In both studies the single OH-stretching band for the pure Si end-member phase shifts about 42 cm^{-1} to lower frequencies, as Si is completely exchanged for Ge. Furthermore, in both studies the FWHM of the Ge end-member phase is noticeably smaller than that of the Si end-member. The fact that both amphibole and talc experience the same frequency shift with the substitution of Ge for Si suggests that the same basic process is occurring in both minerals, namely an increase in the degree of hydrogen bonding with increasing Ge content as proposed above. The main difference between this study and that of Martin et al. (1996) is in the spectra of the intermediate compositions; in this study there is a relatively simple and continuous shift of the OH-stretching band to lower frequencies, whereas in Si-Ge-talc solid solutions there is considerable band broadening and complexity

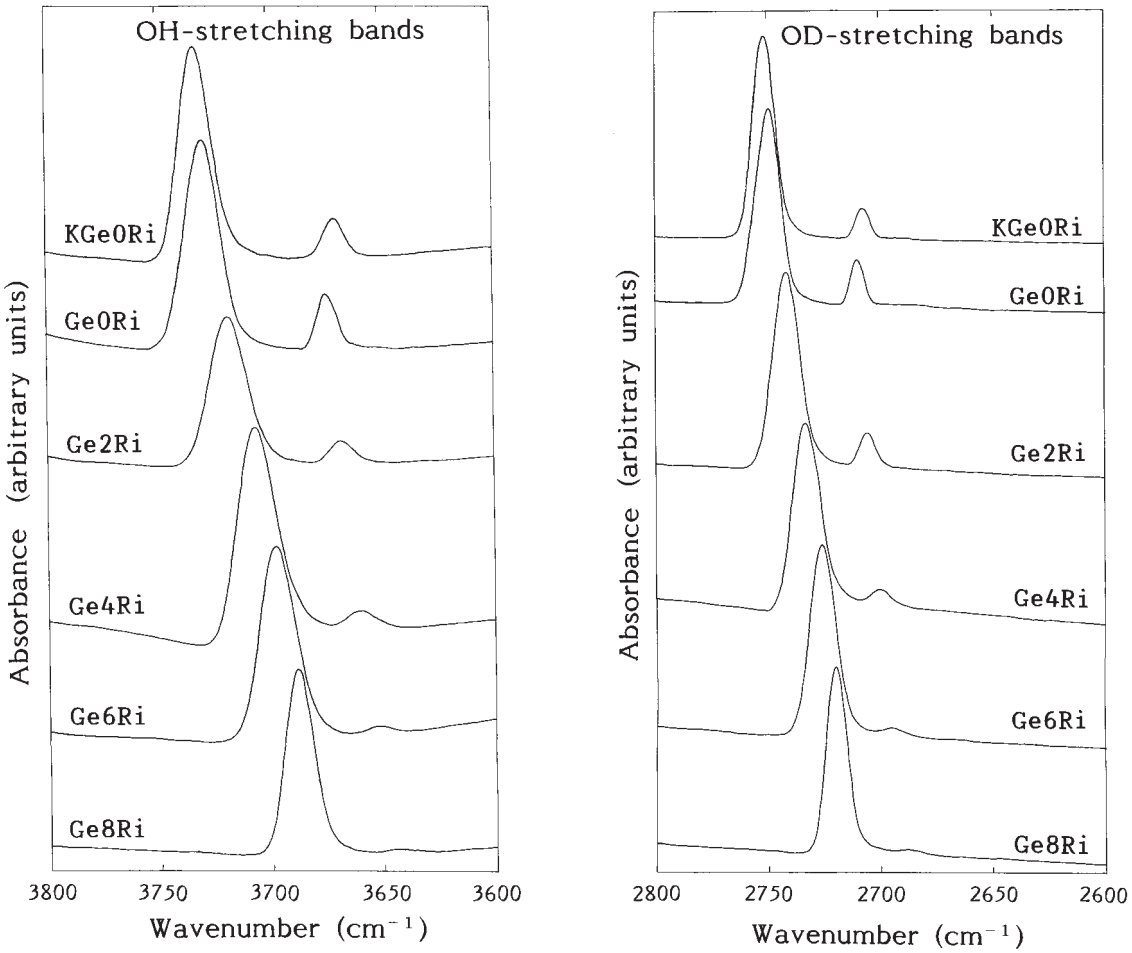

FIGURE 6. Infrared OH/OD-stretching bands for synthesized Si-Ge richterites. (**a**) OH-stretching bands. (**b**) OD-stretching bands.

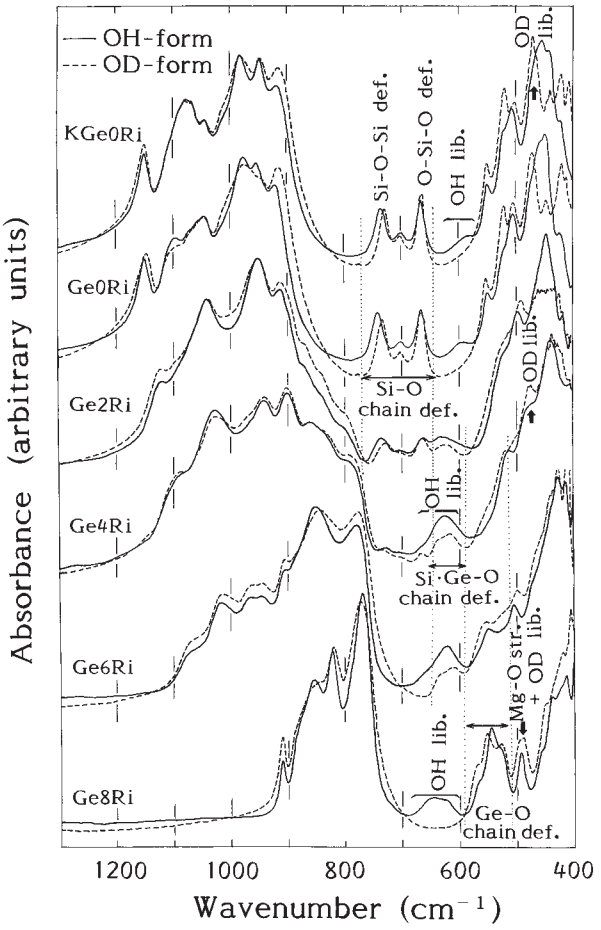

FIGURE 7. IR spectra in the lattice vibration region.

in the spectra. Martin et al. (1996) attributed the band complexity in the intermediate talc compositions to the presence of individual resolvable bands which they assigned to five different tetrahedral cation configurations. Such individual bands were not observed for the Si-Ge-richterite solid solutions studied here, indicating that some difference must exist between the influence of Ge on the OH-stretching frequencies of layered silicates compared to A-site filled double-chain silicates that is not yet understood.

ACKNOWLEDGMENTS

We thank I. Shinno and T. Isobe for their helpful comments. The original manuscript was greatly improved by the reviews of M. Gottschalk and G. Della Ventura. We also appreciate help from Y. Kuwahara and T. Morimura for the SEM and TEM-EDS analyses. Thanks are given to W. Blackburn for help with the electron microprobe analyses. D.M.J. acknowledges NSF grant 0228975 for partial support for this research. Infrared spectra were recorded at the Center of Advanced Instrumental Analysis, Kyushu University.

REFERENCES CITED

Andrut, M., Gottschalk, M., Melzer, S., and Najorka, J. (2000) Lattice vibrational modes in synthetic tremolite-Sr-tremolite and tremolite-richterite solid solutions. Physics and Chemistry of Minerals, 27, 301–309.

Cameron, M., Sueno, S., Papike, J.J., and Prewitt, C.T. (1983) High temperature crystal chemistry of K and Na fluor-richterites. American Mineralogist, 68, 924–943.

Charles, R.W. (1975) The phase equilibria of richterite and ferrorichterite. American Mineralogist, 60, 367–374.

Della Ventura, G., Robert, J.-L., Raudsepp, M., and Hawthorne, F.C. (1993a) Site occupancies in monoclinic amphiboles: Rietveld structure refinement of synthetic nickel magnesium cobalt potassium richterite. American Mineralogist, 78, 633–640.

Della Ventura, G., Robert, J.-L., Beny, J.M., Raudsepp, M., and Hawthorne, F.C. (1993b) The OH-F substitution in Ti-rich richterite: Rietveld structure refinement and FTIR and micro-Raman spectroscopic studies of synthetic amphiboles in the system K_2O-Na_2O-CaO-MgO-SiO_2-TiO_2-H_2O-HF. American Mineralogist, 78, 980–987.

Della Ventura, G., Robert, J.-L., Hawthorne, F.C., and Prost, R. (1996a) Short-range disorder of Si and Ti in the tetrahedral double-chain unit of synthetic Ti-bearing potassium-richterite. American Mineralogist, 81, 56–60.

Della Ventura, G., Robert, J.-L., and Hawthorne, F.C. (1996b) Infrared spectroscopy of synthetic (Ni,Mg,Co)-potassium-richterite. In M.D Dyar, C. McCammon, and M.W. Schaefer, Eds., Mineral Spectroscopy: A Tribute to Roger G. Burns, p. 55–63. The Geochemical Society Special Publication No. 5.

Della Ventura, G., Robert, J.-L., Raudsepp, M., Hawthorne, F.C., and Welch, M.D. (1997) Site occupancies in synthetic monoclinic amphiboles: Rietveld structure refinement and infrared spectroscopy of (nickel, magnesium, cobalt)-richterite. American Mineralogist, 82, 291–301.

Della Ventura, G., Hawthorne, F.C., Robert, J.-L., Delbove, F., Welch, M.F., and Raudsepp, M. (1999) Short-range order of cations in synthetic amphiboles along the richterite-pargasite join. European Journal of Mineralogy, 11, 79–94.

Farmer, V.C. (1975) Infra-red spectroscopy in mineral chemistry. In A.W. Nicol, Ed., Physicochemical methods of mineral analysis, p. 357–388. Plenum Press, New York.

Gillet, P., Reynard, B., and Tequi, C. (1989) Thermodynamic properties of glaucophane: new data for calorimetric and spectroscopic measurements. Physics and Chemistry of Minerals, 16, 659–669.

Gottschalk, M. and Andrut, M. (1998) Structural and chemical characterization of synthetic (Na,K)-richterite solid solutions by EMP, HTREM, XRD, and OH-valence vibrational spectroscopy. Physics and Chemistry of Minerals, 25, 101–111.

Hawthorne, F.C., Della Ventura, G.D., Robert, J.-L., Welch, M.D., Raudsepp, M., and Jenkins, D.M. (1997) A Rietveld and infrared study of synthetic amphiboles along the potassium-richterite-tremolite join. American Mineralogist, 82, 708–716.

Ishida, K. (1990) Identification of infrared OH librational bands of talc-willemseite solid solutions and $Al^{(IV)}$-free amphiboles through deuteration. Mineralogical Journal, 15, 93–104.

Izumi, F. and Ikeda, T. (2000) Multi-purpose pattern-fitting system RIETAN- 2000 and its applications to microporous materials. Journal of the Crystallographic Society of Japan, 42, 516–521.

Jenkins, D.M. (1989) Empirical study of the infrared lattice vibrations (1100–350 cm^{-1}) of phlogopite. Physics and Chemistry of Minerals, 16, 408–414.

Langer, K. and Lattard, D. (1980) Identification of a low-energy OH-valence vibration in zoisite. American Mineralogist, 65, 779–783.

Lazarev, A.N. (1972) Vibrational spectra and structure of silicates. Consultants Bureau (Division of Plenum Publishing Corporation), New York.

Libowitzky, E. (1999) Correlation of O-H stretching frequencies and O-H···O hydrogen bond lengths in minerals. Monatshefte für Chemie, 130, 1047–1059.

Martin, F., Ildefonse, P., Hazemann, J.-L., Petit, S., Grauby, O., and Decarreau, A. (1996) Random distribution of Ge and Si in synthetic talc: an EXAFS and FTIR study. European Journal of Mineralogy, 8, 289–299.

Melzer, S., Gottschalk, M., Andrut, M., and Heinrich, W. (2000) Crystal chemistry of K-richterite–richterite–tremolite solid solutions: a SEM, EMP, XRD, HRTEM and IR study. European Journal of Mineralogy, 12, 273–291.

Pawley, A.R., Graham, C.M., and Navrotsky, A. (1993) Tremolite-richterite amphiboles: Synthesis, compositional and structural characterization and thermochemistry. American Mineralogist, 78, 23–35.

Robert, J.-L., Della Ventura, G.C., and Thauvin, J.-L. (1989) The infrared OH-stretching region of synthetic richiterites in the system Na_2O-K_2O-CaO-MgO-SiO_2-H_2O-HF. European Journal of Mineralogy, 1, 203–211.

Robert, J.-L., Della Ventura, G., Raudsepp, M., and Hawthorne, F.C. (1993) Rietveld structure refinement of synthetic strontium-rich potassium-richterites. European Journal of Mineralogy, 5, 199–206.

Shannon, R.D. (1976) Revised effective ionic radii and systematic studies of interatomic distances in halides and chalcogenides. Acta Crystallographica, A32, 751–767.

Shirozu, H. and Ishida, K (1982) Infrared study of some 7 Å and 14 Å layer silicates by deuteration. Mineralogical Journal, 11, 161–171.

MANUSCRIPT RECEIVED MARCH 12, 2004
MANUSCRIPT ACCEPTED SEPTEMBER 10, 2004
MANUSCRIPT HANDLED BY SIMONA QUARTIERI